RADIO SCIENCE, VOL. 37, NO. 4, 1049, 10.1029/2000RS002551, 2002

High-order high-frequency solutions of rough surface scattering problems

Oscar P. Bruno

Applied Mathematics, California Institute of Technology, Pasadena, California, USA

Alain Sei and Maria Caponi

Ocean Technology Department, TRW, Redondo Beach, California, USA

Received 30 August 2000; revised 12 October 2001; accepted 6 February 2002; published 11 July 2002.

[1] A new method is introduced for the solution of problems of scattering by rough surfaces in the high-frequency regime. It is shown that high-order summations of expansions in inverse powers of the wave number can be used within an integral equation framework to produce highly accurate results for surfaces and wavelengths of interest in applications. Our algorithm is based on systematic use and manipulation of certain Taylor-Fourier series representations and explicit asymptotic expansions of oscillatory integrals. Results with machine precision accuracy are presented which were obtained from computations involving expansions of order as high as 20. *INDEX TERMS:* 0669 Electromagnetics: Scattering and diffraction; 0659 Electromagnetics: Random media and rough surfaces; 0644 Electromagnetics: Numerical methods; 0689 Electromagnetics: Wave propagation (4275); *KEYWORDS:* scattering, rough surface, high frequency, numerical methods, integral equations

1. Introduction

[2] Computations of electromagnetic scattering from rough surfaces play important roles in a wide range of applications, including remote sensing, surveillance, nondestructive testing, etc. The problem of evaluating such scattering returns is rather challenging, owing to the multiple-scale nature of rough scatterers, whose spectra may span a wide range of length scales [*Valenzuela*, 1978].

[3] A number of techniques have been developed to treat limiting cases of this problem. For example, the high-frequency case, in which the wavelength λ of the incident radiation is much smaller than the characteristic surface length scales, has been treated by means of low-order asymptotic expansions, such as the Kirchhoff approximation. On the other hand, resonant problems where the incident radiation wavelength is of the order of the roughness scale have been treated by perturbation methods, typically first- or second-order expansions in the height h of the surface [*Rice*, 1951; *Shmelev*, 1972; *Mitzner*, 1964; *Voronovich*, 1994]. However, when a multitude of scales is present on the surface, none of these techniques is adequate, and attempts to combine them in a so-called two-scale approach have been made [*Kuryanov*, 1963; *McDaniel and Gorman*, 1983; *Voronovich*, 1994; *Gil'Man et al.*, 1996]. The results provided by these methods are not always satisfactory, owing to the limitations imposed by the low orders of approximation used in both the high-frequency and the small-perturbation methods.

[4] A new approach to multiscale scattering, based on use of expansions of very high order in both parameters λ and h, has been proposed recently [*Bruno et al.*, 2000]. These combined methods, which are based on complex variable theory and analytic continuation, require nontrivial mathematical treatments; the resulting approaches, however, do expand substantially on the range of applicability over low-order methods and can be used in some of the most challenging cases arising in applications. Perturbation series of very high order in h have been introduced and used elsewhere to treat resonant problems, in which the wavelength of radiation is comparable to the surface length scales [*Bruno and Reitich*, 1993a, 1993b, 1993c; *Sei et al.*, 1999]. In this paper we focus on our high-order perturbation series in the wavelength λ, which, as we shall show, exhibits excellent convergence in the high-frequency, small-wavelength regime. The combined (h, λ) perturbation algorithms for multiscale surfaces, which require as a main component the accurate high-frequency solvers presented in this paper, are described by *Bruno et al.* [2000].

[5] Our approach to the present high-frequency problem uses an integral equation formulation, whose solution

0148-0227/02/2000RS002551

ν is sought and obtained in the form of an asymptotic expansion

$$\nu(x,\ k) = e^{i\alpha x - i\beta f(x)} \sum_{n=p}^{+\infty} \frac{\nu_n(x)}{k^n}, \tag{1}$$

with $p = -1$ for transverse magnetic (TM) polarization and $p = 0$ for transverse electric (TE) polarization. This expansion is similar in form to the geometrical optics series [*Lewis and Keller*, 1964]

$$u(x,\ y,\ k) = e^{ikS(x,y)} \sum_{n=0}^{+\infty} \frac{u_n(x,y)}{k^n}, \tag{2}$$

where $S = S(x, y)$ is the unknown phase of the scattered field. Note that the phase of the density ν of equation (1) is determined directly from the geometry and the incident field and, unlike that in the geometrical optics field, it is not an unknown of the problem. In particular, the present approach does not require solution of an eikonal equation [*Vidale*, 1988; *VanTrier and Symes*, 1991; *Fatemi et al.*, 1995; *Benamou*, 1999], and it bypasses the complex nature of the field of rays, caustics, etc.

[6] The validity of the expansion (2) has been extensively studied [*Friedlander*, 1946; *Luneburg*, 1944, 1949a, 1949b; *Van Kampen*, 1949]; in particular, it is known that equation (2) needs to be modified in the presence of singularities of the scattering surface. To treat edges and wedges, for example, an expansion containing powers of $k^{-1/2}$ [*Luneburg*, 1949b; *Van Kampen*, 1949; *Keller*, 1958; *Lewis and Boersma*, 1969; *Lewis and Keller*, 1964] must be used; caustics and creeping waves also lead to similar modified expansions [*Kravtsov*, 1964; *Brown*, 1966; *Ludwig*, 1966; *Lewis et al.*, 1967; *Ahluwalia et al.*, 1968]. Proofs of the asymptotic nature of expansion (2) were given in cases where no such singularities occur [*Miranker*, 1957; *Bloom and Kazarinoff*, 1976]. In practice, only expansions (2) of very low orders (one or, at most, two) have been used, owing in part to the substantial algebraic complexity required by high-order expansions [*Bouche et al.*, 1997]. First-order versions of expansion (1), on the other hand, were treated by *Lee* [1975], *Chaloupka and Meckelburg* [1985], and *Ansorge* [1986, 1987].

[7] The region of validity of our asymptotic expression (1), on the other hand, corresponds to configurations where no shadowing occurs. At shadowing, the wave vector of the incident plane wave is tangent to the surface at some point, which causes certain integrals to diverge; see section 4. Thus a different kind of expansion, in fractional powers of $1/k$, should be used to treat shadowing configurations: A first-order version of such an expansion was discussed by *Hong* [1967]; see *Friedlander and Keller* [1955], *Lewis and Keller* [1964], *Brown* [1966], and *Duistermaat* [1992] for the ray-tracing counterpart.

[8] In this paper we show that high-order summations of expansion (1) can indeed be used to produce highly accurate results for surfaces and wavelengths of interest in applications for both TE and TM polarizations; in section 7, for example, we present results with machine precision accuracy, which were obtained from computations involving expansions of order as high as 20. Our algorithm is based on systematic use and manipulation of certain Taylor-Fourier series representations, which we discuss in section 5. Operations such as product, composition, and inversion of Taylor-Fourier series lie at the core of our algebraic treatment; as shown in section 5, certain numerical subtleties associated with these operations require a careful treatment for error control.

[9] In order to streamline our discussion we first treat, in sections 2–5, the complete formalism in the TE case; the changes necessary for the TM case are then described in section 6. In detail, in section 2 we present our basic recursive formula for the evaluation of the coefficients $\nu_n(x)$ of equation (1) for the TE case. These coefficients depend on certain explicit asymptotic expansions of integrals, which we present in sections 3 and 4. A discussion of the Taylor-Fourier algebra then ensues in section 5. As we said, the modifications necessary for the TM case are discussed in section 6. A variety of numerical results for both TE and TM polarizations, finally, are presented in section 7.

2. High-Frequency Integral Equations: TE Case

[10] The scattered field $u = u(x, y)$ induced by an incident plane wave impinging on the rough surface $y = f(x)$ under TE polarization is the solution of the Helmholtz equation with a Dirichlet boundary condition. As is known [*Voronovich*, 1994], the field $u(x, y)$ can be computed as an integral involving a surface density $\nu(x, k)$ and the Green's function $G(x, y, x', y')$ for the Helmholtz equation

$$u(x,y) = \int_{-\infty}^{+\infty} \nu(x',k) \frac{\partial G}{\partial n'}[x,y,x',f(x')] \sqrt{1+[f'(x')]^2}\, dx', \tag{3}$$

where ν satisfies the boundary integral equation

$$\frac{\nu(x,k)}{2} + \int_{-\infty}^{+\infty} \frac{\partial G}{\partial n'}[x,f(x),x',f(x')] \cdot \sqrt{1+[f'(x')]^2}\,\nu(x',k)\,dx' = -e^{i\alpha x - i\beta f(x)}. \tag{4}$$

In what follows we will use the relations

$$\frac{\partial G}{\partial n'}[x,f(x),x',f(x')]\sqrt{1+[f'(x')]^2} = -\frac{i}{4}h(kr)g(x,x'),$$
$$r = \sqrt{(x'-x)^2+[f(x')-f(x)]^2},\ h(t) = tH_1^1(t),$$
$$g(x,x') = \frac{f(x')-f(x)-(x'-x)f'(x')}{r^2},\ \alpha = k\sin(\theta),$$
$$\beta = k\cos(\theta),$$

where H_1^1 is the Hankel function, θ is the incidence angle measured counterclockwise from the vertical axis, and $k = 2\pi/\lambda$ is the wave number.

[11] A useful form of the integral equation (4) results as we factor out the rapidly oscillating phase function $e^{i\alpha x - i\beta f(x)}$

$$\left[e^{-[i\alpha x - i\beta f(x)]}\nu(x,k)\right] - \frac{i}{2}\int_{-\infty}^{+\infty} h(kr)g(x,x') \cdot \left[e^{-[i\alpha x - i\beta f(x)]}\nu(x',k)\right]dx' = -2, \quad (5)$$

which cancels the fast oscillations in all nonintegrated terms and thus suggests use of an asymptotic expression of the form

$$\nu(x,k) = e^{i\alpha x - i\beta f(x)}\sum_{n=0}^{+\infty}\frac{\nu_n(x)}{k^n}. \quad (6)$$

Substitution of the asymptotic expression (6) into equation (5) then yields

$$\sum_{n=0}^{+\infty}\frac{1}{k^n}\left[\nu_n(x) - \frac{i}{2}I^n(x,k)\right] = -2, \quad (7)$$

where

$$I^n(x,k) = \int_{-\infty}^{+\infty} h(kr)g(x,x')\exp\{i\alpha(x'-x) - i\beta[f(x')-f(x)]\}\nu_n(x')dx'.$$

To solve equation (7), we use asymptotic expansions for the integrals $I^n(x, k)$, collect coefficients of each power of $1/k$, and then determine, recursively, the coefficients $\nu_n(x)$. In detail, we obtain in section 3 an expansion which gives $I^n(x, k)$ in terms of derivatives of $\nu_n(x)$

$$I^n(x,k) = \frac{1}{k}\sum_{q=0}^{+\infty}\frac{I_q^n(x)}{k^q} \quad I_q^n(x) = \sum_{\ell=0}^{q}\frac{\partial^\ell \nu_n(x)}{\partial x^\ell}B_{q-\ell}(x), \quad (8)$$

where the functions $B_{q-l}(x)$ are determined from the profile and incidence angle only. (We point out, however, that our algebraic treatment yields an expression for $I_q^n(x)$ which, although equivalent to that of equation (8), is different in form; see section 3 and equation (25).) From equations (7) and (8) we then find a recursion which gives $\nu_n(x)$ as a linear combination of derivatives of the previous coefficients $\nu_{n-1-q}(x)$

$$\begin{cases} \nu_0(x) = -2 \\ \nu_n(x) = \dfrac{i}{2}\displaystyle\sum_{q=0}^{n-1} I_q^{n-1-q}(x). \end{cases} \quad (9)$$

Use of the Taylor-Fourier algebra of section 5 allows us to perform accurately the high-order differentiations required by our high-order expansions; the needed expansion (8) of the integral I^n, in turn, is the subject of section 3.

3. Asymptotic Expansion of $I^n(x, k)$

[12] We first split the integral I^n as a sum $I^n = I_-^n + I_+^n$ where

$$I_-^n(x,k) = \int_{-\infty}^{x} h(kr)g(x,x')\exp\{i\alpha(x'-x) - i\beta[f(x')-f(x)]\}\nu_n(x')dx',$$
$$I_+^n(x,k) = \int_{x}^{+\infty} h(kr)g(x,x')\exp\{i\alpha(x'-x) - i\beta[f(x')-f(x)]\}\nu_n(x')dx'.$$

We evaluate in detail the asymptotic expansion for $I_+^n(x, k)$; the corresponding expansion for I_-^n then follows analogously.

[13] Using $t = x' - x$, we obtain

$$I_+^n(x,k) = \int_0^{+\infty} h[k\phi_+(x,t)]g(x,x+t)\exp\{i\alpha t - i\beta \cdot [f(x+t)-f(x)]\}\nu_n(x+t)dt, \quad (10)$$

where

$$\phi_+(x,t) = \sqrt{t^2+(f(x+t)-f(x))^2}.$$

For the treatment presented here, $f(x)$ is assumed to satisfy the condition

$$\phi_+'(x,t) = \frac{\partial\phi_+(x,t)}{\partial t} > 0 \qquad t \geq 0 \quad (11)$$

so that the map $t \mapsto \phi_+(x, t)$ is invertible. (This condition is generally satisfied by rough surfaces considered in practice: For a sinusoidal profile $f(x) = a\cos(x)$, for example, the inequality (11) holds as long as $a < 1$). Then setting

$$u = \phi_+(x,t) \iff t = \phi_+^{-1}(x,u),$$

equation (10) becomes

$$I_+^n(x,k) = \int_0^{+\infty} h(ku)\frac{g[x, x+\phi_+^{-1}(x,u)]}{\phi_+'[x,\phi_+^{-1}(x,u)]}\nu_n \cdot [x+\phi_+^{-1}(x,u)]\exp(i\alpha\phi_+^{-1}(x,u) - i\beta\{f[x+\phi_+^{-1}(x,u)] - f(x)\})du.$$

Calling

$$\begin{cases} F_+^n(x,u) = \frac{g[x,x+\phi_+^{-1}(x,u)]}{\phi_+'[x,\phi_+^{-1}(x,u)]}\nu_n[x+\phi_+^{-1}(x,u)] \\ \psi_+(x,u) = \{f[x+\phi_+^{-1}(x,u)] - f(x)\}\cos(\theta) - \phi_+^{-1}(x,u)\sin(\theta), \end{cases} \tag{12}$$

$I_+^n(x, k)$ reduces to

$$I_+^n(x,k) = \int_0^{+\infty} F_+^n(x,u)h(ku)e^{-ik\,\psi_+(x,u)}du.$$

The unknown $\nu_n(x)$ is contained as a factor in the function $F_+^n(x, u)$. Notation (12) is useful in that it helps present the integrand as a product of two distinct factors: a nonoscillatory component $F_+^n(x, u)$ and an oscillatory component $h(ku)e^{-ik\psi_+(x,u)}$.

[14] In addition to equation (11) we assume that the profile $y = f(x)$ is an analytic function, so that the map $u \mapsto F_+^n(x, u)$ is analytic as well. Using the Taylor series

$$F_+^n(x,u) = \sum_{m=0}^{+\infty}\frac{\partial^m F_+^n(x,0)}{\partial u^m}\frac{u^m}{m!} = \sum_{m=0}^{+\infty} p_{n,m}^+(x)u^m, \tag{13}$$

the integral $I_+^n(x, k)$ takes the form

$$I_+^n(x,k) = \sum_{m=0}^{+\infty} p_{n,m}^+(x)\int_0^{+\infty} u^m h(ku)e^{-ik\,\psi^+(x,u)}du = \sum_{m=0}^{+\infty}\frac{p_{n,m}^+(x)}{k^{m+1}}\int_0^{+\infty} v^m h(v)e^{-ik\,\psi^+(x,v/k)}dv. \tag{14}$$

Thus the $1/k$ expansion of I_+^n results from the corresponding expansions of the integrals

$$A^+(k,m,x) = \int_0^{+\infty} v^m h(v)e^{-ik\,\psi^+(x,v/k)}dv. \tag{15}$$

These nonconvergent integrals must be reinterpreted by means of analytic continuation, in a manner similar to that used in the definition and manipulation of Mellin transforms [*Bleistein and Handelsman*, 1986]. An explicit expansion of $A^+(k, m, x)$ is given in section 3.1.

3.1. Expansion of the Integrals I_+^n and I_-^n

[15] Using the Taylor expansion of

$$\psi^+(x,u) = \sum_{m=0}^{+\infty}\psi_m^+(x)\frac{u^m}{m!}$$

in the variable u together with the identity $\psi^+(x, 0) = 0$, expansion of the function $\exp\{-i[k\psi^+(x,(v/k) - \psi_1^+(x)v]\}$ leads to the expression

$$e^{-ik\psi^+(x,v/k)} = e^{-i\psi_1^+(x)v}\left(1 + \sum_{n=1}^{+\infty}k^{-n}\sum_{\ell=1}^{n}\frac{a_{\ell,n}^+(x)}{\ell!}v^{n+\ell}\right) \tag{16}$$

for certain (function) coefficients $a_{l,n}^+(x)$. Then, defining

$$A_0^+(p,x) = \int_0^{+\infty} v^p h(v)e^{-i\psi_1^+(x)v}dv, \tag{17}$$

$$A_n^+(m,x) = \sum_{\ell=0}^{n}\frac{a_{\ell,n}^+(x)}{\ell!}A_0^+(m+n+\ell,x), \tag{18}$$

we obtain

$$A^+(k,m,x) = A_0^+(m,x) + \sum_{n=1}^{+\infty}\frac{A_n^+(m,x)}{k^n} \tag{19}$$

and the series

$$I_+^n(x,k) = \sum_{q=0}^{+\infty}\left(\sum_{\ell=0}^{q}p_{n,q-\ell}^+(x)A_\ell^+(q-\ell,x)\right)k^{-q-1} \tag{20}$$

for I_+^n results. We see that this expansion is given in terms of the integrals (17), which, like those of equation (15), are nonconvergent and require analytic continuation. An explicit expression for this integral as a function of p and x is given in section 4.

[16] The case of $I_-^n(x, k)$ can be treated similarly: We use $t = x - x'$ and the definitions

$$\phi_-(x,t) = \sqrt{t^2 + [f(x-t) - f(x)]^2},$$

$$F_-^n(x,u) = \frac{g[x,x-\phi_-^{-1}(x,u)]}{\phi_-'[x,\phi_-^{-1}(x,u)]}\nu_n[x-\phi_-^{-1}(x,u)],$$

$$\psi^-(x,u) = \{f[x-\phi_-^{-1}(x,u)] - f(x)\}\cos(\theta) - \phi_-^{-1}(x,u)\sin(\theta).$$

Then, letting $a_{l,n}^-(x)$ be the coefficients in the expansion of $e^{-ik\nu\psi^-(x,v/k)}$

$$e^{-ik\psi^-(x,v/k)} = e^{-i\psi_1^-(x)v}\left(1 + \sum_{n=1}^{+\infty}k^{-n}\sum_{\ell=1}^{n}\frac{a_{\ell,n}^-(x)}{\ell!}v^{n+\ell}\right),$$

calling

$$A_0^-(p,x) = \int_0^{+\infty} v^p h(v)e^{-i\psi_1^-(x)v}dv,$$

and defining the functions $A_n^-(m, x)$ by

$$A_n^-(m,x) = \sum_{\ell=0}^{n} \frac{a_{\ell,n}^-(x)}{\ell!} A_0^-(m+n+\ell,x), \qquad (21)$$

we obtain the expansion for the integral I_-^n:

$$I_-^n(x,k) = \sum_{q=0}^{+\infty} \left(\sum_{\ell=0}^{q} p_{n,q-\ell}^-(x) A_\ell^-(q-\ell,x) \right) k^{-q-1}. \quad (22)$$

3.2. A Simplified Expression for the Integral $I^n(x, k)$

[17] The expansions for $I_+^n(x, k)$ and $I_-^n(x, k)$ can be combined into an expression which depends only on the functions $p_{n,l}^+(x)$, $a_{l,n}^+(x)$, and

$$S(q,x) = A_0^+(q,x) + (-1)^q A_0^-(q,x). \qquad (23)$$

Indeed, using the identity $\phi^-(x, t) = \phi^+(x, -t)$, we find

$$\psi_\ell^-(x) = (-1)^\ell \psi_\ell^+(x), \quad a_{\ell,n}^-(x) = (-1)^{\ell+n} a_{\ell,n}^+(x),$$
$$p_{n,\ell}^-(x) = (-1)^\ell p_{n,\ell}^+(x). \qquad (24)$$

The $1/k$-expansion of $I^n(x, k)$ now follows from equations (20), (22), and (24)

$$\begin{aligned} I^n(x,k) &= I_+^n(x,k) + I_-^n(x,k) \\ &= \sum_{q=0}^{+\infty} \left(\sum_{\ell=0}^{q} p_{n,q-\ell}^+(x) A_\ell^+(q-\ell,x) + p_{n,q-\ell}^-(x) \right. \\ &\quad \left. \cdot A_\ell^-(q-\ell,x) \right) k^{-q-1} \\ &= \sum_{q=0}^{+\infty} \sum_{\ell=0}^{q} p_{n,q-\ell}^+(x) \left(A_\ell^+(q-\ell,x) + (-1)^{q-\ell} \right. \\ &\quad \left. \cdot A_\ell^-(q-\ell,x) \right) k^{-q-1}. \end{aligned}$$

Using equations (18), (21), and (24), we thus obtain our key formula

$$I^n(x,k) = \sum_{q=0}^{+\infty} \frac{I_q^n(x)}{k^{q+1}}$$
$$I_q^n(x) = \sum_{\ell=0}^{q} p_{n,q-\ell}^+(x) \left(\sum_{j=0}^{\ell} \frac{a_{j,\ell}^+(x)}{\ell!} S(q+j,x) \right). \qquad (25)$$

[18] As we have seen, the function $S(m, x)$ is defined by divergent integrals; an explicit expression for this function is given in section 4. The coefficients $a_{j,m}^+$ and $p_{n,m}^+$, in turn, are defined as products, quotients, compositions, and inverses of certain power series expansions; accurate methods for such manipulations of power series are given in section 5. Note that $a_{j,l}^+(x)$ and $S(q + j, x)$ depend on the scattering profile and incidence angle only; the coefficient $p_{n,m}^+$ depends on the geometry and the derivatives of the coefficient ν_n of order $\leq m$.

4. Computation of $S(q, x)$

[19] Interestingly, a closed-form expression can be given for the function $S(q, x)$. Indeed, since $\psi_1^-(x) = \psi_1^+(x)$, we may write

$$\begin{aligned} S(q,x) &= A_0^+(q,x) + (-1)^q A_0^-(q,x) \\ &= \int_0^{+\infty} v^q h(v) \left(e^{-i\psi_1^+(x)v} + (-1)^q e^{i\psi_1^+(x)v} \right) dv, \end{aligned}$$

or

$$S(q,x) = \begin{cases} 2\displaystyle\int_0^{+\infty} v^{q+1} H_1^1(v) \cos[\psi_1^+(x)v]\, dv & q \text{ even} \\ -2i\displaystyle\int_0^{+\infty} v^{q+1} H_1^1(v) \sin[\psi_1^+(x)v]\, dv & q \text{ odd.} \end{cases}$$

Using formulas (11.4.19) and (11.4.16) of *Abramowitz and Stegun* [1964] together with the Taylor expansion of sin (x) and cos (x), we then obtain the closed-form expression

$$S(q,x) = \begin{cases} 2^{q+2} \displaystyle\sum_{k=0}^{+\infty} (-1)^k \frac{[2\psi_1^+(x)]^{2k}}{(2k)!} \frac{\Gamma\left(\frac{2k+q+3}{2}\right)}{\Gamma\left(\frac{1-2k-q}{2}\right)} & q \text{ even} \\ -i\, 2^{q+2} \displaystyle\sum_{k=0}^{+\infty} (-1)^k \frac{[2\psi_1^+(x)]^{2k+1}}{(2k+1)!} \frac{\Gamma\left(\frac{2k+q+4}{2}\right)}{\Gamma\left(\frac{-2k-q}{2}\right)} & q \text{ odd.} \end{cases} \qquad (26)$$

Thus $S(q, x)$ is a series in powers of $\psi_1^+(x)$, whose coefficients can be evaluated explicitly in terms of the Γ function.

[20] It is easy to see that the radius of convergence of the power series in equation (26) is 1 and that the series actually diverges for $\psi_1^+ = 1$. This condition has an interesting physical interpretation; since

$$\psi_1^+(x) = \frac{f'(x)\cos(\theta) - \sin(\theta)}{\sqrt{1+f'(x)^2}},$$

the condition $\psi_1^+(x) = 1$ is equivalent to

$$f'(x) = -\cot(\theta)$$

or, equivalently, some rays in the incident plane wave are tangent to the scattering surface. Alternatively, using the asymptotic expansion

$$H_1^1(v) \sim \sqrt{\frac{2}{\pi v}} \exp\left\{ i\left(v - \frac{3\pi}{4} \right) \right\},$$

Table 1. Values of the Derivatives of the Function $S(x)$ at $x = 0$ for Various Orders of Differentiation[a]

		20 Modes		30 Modes		40 Modes	
Order	Exact Value at 0	FFT	Conv.	FFT	Conv.	FFT	Conv.
2	−7.376924249352232e-01	1.3e-12	5.4e-16	1.7e-11	2.7e-16	1.0e-11	2.7e-16
4	2.377008924791275e+00	6.8e-11	3.0e-14	4.2e-09	2.9e-15	9.8e-10	2.9e-15
6	−1.702966504696142e+01	5.5e-10	1.8e-12	4.6e-07	0.0e-00	1.7e-07	0.0e-00
8	2.184589621949499e+02	2.7e-08	5.8e-11	2.9e-05	2.3e-15	4.1e-05	2.3e-15
10	−4.361708943655447e+03	8.8e-07	1.2e-09	1.1e-03	6.9e-16	3.8e-03	6.9e-16
12	1.248619506829422e+05	1.4e-05	1.7e-08	3.1e-02	0.0e-00	2.2e-01	8.0e-16
14	−4.844671808314213e+06	1.4e-04	1.8e-07	6.5e-01	6.0e-15	8.7e+00	1.0e-15
16	2.445839768254340e+08	1.1e-03	1.5e-06	1.0e+01	1.3e-13	2.7e+02	1.6e-15
18	−1.557531553377787e+10	6.5e-03	9.4e-06	1.3e+02	1.9e-12	6.6e+03	0.0e-00
20	1.220898732494702e+12	3.1e-02	5.0e-05	1.4e+03	2.2e-11	1.3e+05	8.2e-16

[a] The columns marked "20 modes," "30 modes," and "40 modes" list the relative errors of the derivatives computed by summing differentiated Fourier series truncated at 20, 30, and 40 modes, respectively. Columns FFT and Conv. resulted from use of Fourier coefficients obtained through FFTs and direct convolution, respectively. Read −7.376924249352232e-01 as $-7.376924249352232 \times 10^{-1}$.

we see that the oscillatory term in $A_0^+(p, x)$ is $e^{i\left[1-\psi_1^+(x)\right]\nu}$, which becomes nonoscillatory for $\psi_1^+(x) = 1$ and thus causes the integral to diverge. Therefore, as mentioned in the introduction, the present algorithm applies only to configurations for which no shadowing occurs. Extensions of these methods to configurations including shadowing are forthcoming.

[21] In addition to the infinite series (26), the function S admits a finite closed-form representation, namely,

$$S(q, \psi) = (1 - \psi^2)^{-(q+3/2)} P_q(\psi),$$

where $P_q(x)$ is a polynomial of degree equal to the integer part of $q/2$. These polynomials can be computed easily and efficiently through a Taylor expansion of the product $S(q, \psi)\ (1-\psi^2)^{(q+3/2)}$. For example, for the first few values of q we have

$$S(0, \psi) = (1 - \psi^2)^{-3/2} \cdot 2,$$
$$S(1, \psi) = (1 - \psi^2)^{-5/2}(-6),$$
$$S(2, \psi) = (1 - \psi^2)^{-7/2}(-6 + 24\psi),$$
$$S(3, \psi) = (1 - \psi^2)^{-9/2}(90 + 120\psi),$$
$$S(4, \psi) = (1 - \psi^2)^{-11/2}(90 + 1080\psi + 720\psi^2),$$
$$S(5, \psi) = (1 - \psi^2)^{-13/2}(-3150 - 12,600\psi - 5040\psi^2).$$

5. Computation of $p^+_{n,q-l}$ and $a^+_{j,l}$: Taylor-Fourier Algebra

[22] As indicated previously in section 3, the functions $p^+_{n,q-l}$ and $a^+_{j,l}$ in equations (12), (13), and (16) can be obtained through manipulations of Taylor−Fourier series, which we define, quite simply, as Taylor series whose coefficients are Fourier series. Thus a Taylor-Fourier series $f(x, t)$ is given by an expression of the form

$$f(x,t) = \sum_{n=0}^{+\infty} f_n(x) t^n \quad f_n(x) = \sum_{\ell=-\infty}^{\infty} f_{n\ell}\, e^{i\ell x}. \qquad (27)$$

The manipulations required by our methods include sum, products, and composition, as well as algebraic and functional inverses. These operations need to be implemented with care, as we show in what follows.

Table 2. Results for the Profile of Figure 1a in TE Polarization With $h = 0.025$, $\lambda = 0.025$, and Incidence Angle $\theta = 30°$[a]

Efficiency	Scattered Energy	Order 0	Order 1	Order 5	Order 11	Order 17
0	7.538669511479800e-04	3.8e-02	6.3e-05	1.1e-08	5.0e-12	2.4e-13
1	1.194293110668300e-01	2.0e-04	3.1e-06	4.9e-09	2.8e-13	2.2e-14
2	4.713900020760300e-03	1.5e-02	1.7e-05	2.7e-08	6.5e-13	3.3e-14
3	9.472951023686101e-02	2.4e-03	5.8e-05	1.7e-09	1.2e-13	4.0e-15
4	1.606247510782500e-01	1.2e-04	8.9e-05	2.8e-10	7.3e-14	8.6e-15
5	8.121747375826800e-02	1.5e-03	1.3e-04	2.3e-08	3.5e-14	7.9e-15
6	2.068175899532900e-02	2.7e-03	1.9e-04	1.2e-08	3.1e-13	4.4e-15
7	3.171379802403400e-03	3.9e-03	2.5e-04	3.5e-08	1.5e-13	5.3e-15

[a] The run time was 10 s for the calculation of order 17.

Table 3. Results for the Profile of Figure 1a in TM Polarization With $h = 0.025$, $\lambda = 0.0251$, and Incidence Angle $\theta = 30°$[a]

Efficiency	Scattered Energy	Order 0	Order 1	Order 5	Order 11	Order 17
0	1.148002904781718e-03	3.1e-02	3.4e-05	2.6e-09	7.2e-13	4.0e-13
1	1.196487185464779e-01	1.5e-04	1.1e-05	2.2e-11	1.8e-14	3.3e-14
2	3.930863630633380e-03	1.6e-02	2.9e-05	2.8e-10	1.5e-13	1.1e-13
3	9.729981709870275e-02	2.4e-03	2.3e-05	2.6e-10	4.3e-14	3.7e-14
4	1.603959300090739e-01	1.4e-04	4.0e-05	3.6e-10	1.9e-14	2.4e-14
5	7.991729015156721e-02	1.5e-03	6.5e-05	2.8e-10	1.3e-14	6.9e-15
6	2.011674295356339e-02	2.7e-04	9.8e-05	3.4e-10	4.0e-14	1.3e-14
7	3.052813099869383e-03	3.9e-03	1.4e-04	2.5e-09	4.4e-14	9.6e-14

[a] The run time was 10 s for the calculation of order 17.

[23] Compositions and inverses of Taylor-Fourier series require consideration of multiplication and addition, so we discuss the latter two operations first. Additions do not pose difficulties: Naturally, they result from addition of coefficients. Multiplications and divisions of Taylor-Fourier series, on the other hand, could, in principle, be obtained by means of fast Fourier transforms (FFTs) [*Press et al.*, 1992]. Unfortunately, such procedures are not appropriate in our context. Indeed, as we show below, the very rapid decay of the Fourier and Taylor coefficients arising in our calculations is not well captured through convolutions obtained from FFTs. Since an accurate representation of this decay is essential in our method, which, based on high-order differentiations of Fourier-Taylor series, greatly magnifies high-frequency components, an alternate approach needs to be used.

[24] Before describing our accurate algorithms for manipulation of Taylor-Fourier series, we present an example illustrating the difficulties associated with use of FFTs in this context. We thus consider the problem of evaluating the subsequent derivatives of the function

$$S(x) = \left(\sum_{k=-\infty}^{\infty} \frac{\cos(kx)}{a^{|k|}} \right)^2$$

through multiplication and differentiation of Fourier series. For comparison purposes we note that S actually admits the closed form

$$S(x) = \left(1 + 2 \frac{a \cos(x) - 1}{a^2 - 2a \cos(x) + 1} \right)^2; \qquad (28)$$

the value $a = 10$ is used in the following tests.

[25] In Table 1 we present the errors resulting in the evaluation of a sequence of derivatives of the function S at $x = 0$ through two different methods: FFT and direct summation of the convolution expression. (Here errors were evaluated by comparison with the corresponding values obtained from direct differentiation of expression (28) by means of an algebraic manipulator.) We see that, as mentioned above, use of Fourier series obtained from FFTs leads to substantial accuracy losses. Indeed, FFTs evaluate the small high-order Fourier coefficients of a product through sums and differences of "large" function values, and thus they give rise to large relative errors in the high-frequency components. These relative errors are then magnified by the differentiation process, and all accuracy is lost in high-order differentiations: Note the increasing loss of accuracy that results from use of a larger number of Fourier modes in the FFT procedure. The direct convolution, on the other hand, does not suffer

Table 4. Results for the Profile of Figure 1a in TM Polarization With $h = 0.025$, $\lambda = 0.025$, and Incidence Angle $\theta = 30°$[a]

Efficiency	Scattered Energy	Order 0	Order 1	Order 5	Order 11	Order 17
0	6.978718873398379e-004	4.0e-02	4.8e-05	3.2e-09	4.0e-13	1.6e-15
1	1.193803726254851e-001	2.1e-04	1.1e-05	1.9e-11	1.3e-14	9.3e-16
2	4.854671479355886e-003	1.5e-02	2.5e-05	2.6e-10	3.9e-14	5.4e-16
3	9.427330239288337e-002	2.4e-03	2.3e-05	2.5e-10	6.8e-15	2.9e-16
4	1.606619051666006e-001	1.1e-04	3.9e-05	3.5e-10	4.3e-15	5.2e-16
5	8.146471443830940e-002	1.5e-03	6.4e-05	2.8e-10	4.3e-15	0.0e-16
6	2.079411505463193e-002	2.7e-04	9.6e-05	3.1e-10	2.2e-14	1.0e-15
7	3.195973191313253e-003	3.9e-03	1.4e-04	2.3e-09	1.4e-13	1.9e-15

[a] The run time was 10 s for the calculation of order 17.

Table 5. Results for the Profile of Figure 1b in TE Polarization With $h = 0.01$, $\lambda = 0.025$, and $\theta = 0°$[a]

Efficiency	Scattered Energy	Order 0	Order 1	Order 5	Order 9	Order 11
0	1.983702874853860e-01	1.4e-03	6.7e-06	6.3e-10	1.8e-13	9.8e-16
1	2.125625186015414e-02	4.3e-03	7.3e-06	8.6e-10	4.6e-14	1.5e-14
2	5.109656298137152e-02	4.2e-03	5.3e-06	1.3e-09	3.5e-14	1.1e-14
3	1.350594564861170e-01	1.1e-03	3.0e-06	1.8e-10	5.1e-14	6.6e-15
4	1.670755436364386e-02	4.3e-03	928e-06	1.5e-09	1.8e-13	2.7e-15
5	1.041839113172000e-01	8.7e-04	1.1e-05	4.7e-10	3.8e-14	2.9e-15
6	3.029977474761340e-02	7.6e-04	1.1e-05	4.8e-10	1.0e-15	9.0e-15
7	2.828409217693459e-02	2.5e-03	3.2e-05	1.8e-09	3.5e-14	9.4e-15

[a] The run time was 5 s for the order 11 calculation.

from this difficulty. Indeed, direct convolutions evaluate a particular Fourier coefficient a_n of a product of series through sums of terms of the same order of magnitude as a_n. The result is a series whose coefficients are fully accurate in relative terms, so that subsequent differentiations do not lead to accuracy losses. We point out that full double precision accuracy can be obtained for derivatives of orders 20 and higher provided that sufficiently many modes are used in the method based on direct convolutions.

[26] In addition to sums and multiplications our approach requires use of algorithms for composition as well as algebraic and functional inverses of Taylor-Fourier series. In view of the previous considerations a few comments will suffice to provide a complete prescription. Compositions result from iterated products and sums of Fourier series, and thus they do not present difficulties. As is known from the theory of formal power series [*Cartan*, 1963], functional inverses of a Taylor-Fourier series (27) with $f_0 = 0$ results quite directly once the algebraic inverse of the Fourier series $f_1(x) \neq 0$ is known. We may thus restrict our discussion to evaluation of algebraic inverses of Fourier series.

[27] As in the case of the product of Fourier series, two alternatives can be considered for the evaluation of algebraic inverses. One of them involves point evaluations and FFTs; in view of our previous comments it is clear that such an approach would not lead to accurate numerics. An alternative approach, akin to use of a direct convolution in evaluation of products, requires solution of a linear system of equations for the Fourier coefficients of the algebraic inverse. In view of the decay of the Fourier coefficients of smooth functions, such linear systems can be truncated and solved to produce the coefficients of inverses with high accuracy.

[28] In sum, manipulations of Taylor-Fourier series should not use point-value discretizations if accurate values of functions and their derivatives are to be obtained. The approach described in this section calls, instead, for operations performed fully in Fourier space. In practice we have found that the procedures described here produce full double precision accuracies for all operations between Taylor-Fourier series and their subsequent high-order derivatives in very short computing times.

6. High-Frequency Integral Equations: TM Case

[29] In the transverse magnetic (TM) polarization the scattered field $u = u(x, y)$ induced by an incident plane wave impinging on the rough surface $y = f(x)$ is the solution of the Helmholtz equation with a Neumann boundary condition. The field $u(x, y)$ can be computed [*Voronovich*, 1994] as an integral involving a surface

Table 6. Results for the Profile of Figure 1b in TM Polarization With $h = 0.01$, $\lambda = 0.025$, and $\theta = 0°$[a]

Efficiency	Scattered Energy	Order 0	Order 1	Order 5	Order 9	Order 11
0	1.985778821348800e-01	1.3e-03	1.1e-05	5.6e-11	9.1e-15	5.0e-15
1	2.203189065423864e-02	4.3e-03	6.1e-06	8.5e-12	2.0e-14	2.2e-14
2	4.989624245086630e-02	4.2e-03	1.2e-05	1.3e-10	6.8e-15	8.3e-15
3	1.363942224141270e-01	1.1e-03	3.0e-06	6.6e-11	1.1e-14	6.7e-15
4	1.685456723960805e-02	4.3e-03	1.7e-05	1.5e-10	2.7e-14	1.5e-14
5	1.040033802018770e-01	8.9e-04	9.9e-07	8.4e-11	2.9e-15	2.0e-15
6	2.994981016528542e-02	7.8e-04	1.5e-06	1.9e-10	1.4e-15	1.0e-14
7	2.795532080716518e-02	2.5e-03	1.5e-05	1.2e-11	3.2e-15	1.1e-15

[a] The run time was 4 s for the order 11 calculation.

Table 7. Results for the Profile of Figure 1c in TE Polarization With $h = 0.02$, $\lambda = 0.04$, and $\theta = 0°$[a]

Efficiency	Scattered Energy	Order 0	Order 1	Order 5	Order 11	Order 19
0	2.762105662320035e-01	1.9e-3	1.6e-5	7.4e-9	6.5e-14	2.4e-15
1	5.735818584364873e-02	3.1e-3	2.0e-5	1.9e-8	1.3e-12	6.0e-16
2	9.154897389472935e-02	3.7e-3	5.1e-6	8.2e-9	1.4e-12	6.7e-15
3	1.051875097051952e-01	4.6e-4	5.1e-6	1.6e-9	1.0e-12	9.2e-16
4	6.713521833646909e-02	1.7e-3	2.7e-5	1.4e-11	3.6e-12	2.1e-16
5	2.830374622545111e-02	3.9e-3	7.3e-5	1.4e-8	2.2e-13	6.7e-15
6	9.270117932865375e-03	5.9e-3	1.3e-4	3.2e-8	1.1e-11	3.0e-15
7	2.435385416440963e-03	7.9e-3	2.2e-4	8.4e-8	4.1e-12	1.8e-16

[a] The run time was 27 s for the calculation of order 19.

density $\nu(x, k)$ and the Green's function $G(x, y, x', y')$ for the Helmholtz equation

$$u(x,y) = \int_{-\infty}^{+\infty} \nu(x',k) G[x,y,x',f(x')] \sqrt{1+[f'(x')]^2}\, dx', \tag{29}$$

where ν satisfies the boundary integral equation

$$-\frac{\nu(x,k)}{2} + \int_{-\infty}^{+\infty} \frac{\partial G}{\partial n}[x,f(x),x',f(x')] \sqrt{1+[f'(x')]^2} \cdot \nu(x',k)\, dx' = -\frac{\partial u^{\text{inc}}}{\partial n}[x,f(x)]. \tag{30}$$

In what follows we will use the relations

$$u^{\text{inc}}(x,y) = e^{i\alpha x - i\beta y},\ \frac{\partial G}{\partial n}[x,f(x),x',f(x')] = -\frac{i}{4} h(kr) g(x,x'),$$

$$r = \sqrt{(x'-x)^2 + [f(x')-f(x)]^2},\ h(t) = tH_1^1(t),$$

$$g(x,x') = \frac{f(x)-f(x')-f'(x)(x-x')}{r^2},\quad \alpha = k\sin(\theta),\quad \beta = k\cos(\theta),$$

where H_1^1 is the Hankel function, θ is the incidence angle measured counterclockwise from the vertical axis, and $k = 2\pi/\lambda$ is the wave number. Since

$$\frac{\partial u^{\text{inc}}}{\partial n}[x,f(x)] = -\frac{i\alpha f'(x) + i\beta}{\sqrt{1+[f'(x)]^2}} e^{i\alpha x - i\beta f(x)},$$

calling $\tilde{\nu}(x,k) = \nu(x,k)\sqrt{1+[f'(x)]^2}$, we can rewrite equation (30) as follows:

$$\frac{\tilde{\nu}(x,k)}{2} - \int_{-\infty}^{+\infty} \tilde{\nu}(x',k)\, h(kr) g(x,x')\, dx' = [i\alpha f'(x) + i\beta] e^{i\alpha x - i\beta f(x)}. \tag{31}$$

As in section 2, a useful form of the integral equation (31) results as we factor out the rapidly oscillating phase function $e^{i\alpha x - i\beta f(x)}$

$$\left(e^{-[i\alpha x - i\beta f(x)]}\tilde{\nu}(x,k)\right) - \frac{i}{2}\int_{-\infty}^{+\infty} h(kr) g(x,x') \cdot [e^{-[i\alpha x - i\beta f(x)]}\tilde{\nu}(x',k)]\, dx' = 2[i\alpha f'(x) + i\beta], \tag{32}$$

which cancels the fast oscillations in all nonintegrated terms. Using an expansion for the function $\tilde{\nu}(x, k)$ similar to equation (6)

$$\tilde{\nu}(x,k) = e^{i\alpha x - i\beta f(x)} \sum_{n=-1}^{+\infty} \frac{\nu_n(x)}{k^n} \tag{33}$$

Table 8. Results for the Profile of Figure 1c in TM Polarization With $h = 0.02$, $\lambda = 0.041$, and $\theta = 0°$[a]

Efficiency	Scattered Energy	Order 0	Order 1	Order 5	Order 11	Order 19
0	1.291589358261453e-01	2.2e-03	1.6e-05	2.7e-10	2.1e-12	9.5e-14
1	1.662663939465338e-01	1.7e-03	5.1e-05	2.8e-10	1.6e-12	4.1e-14
2	3.920583564991646e-03	8.5e-03	5.3e-06	7.0e-09	1.3e-11	6.2e-13
3	1.878743087516774e-02	1.5e-02	2.7e-06	2.6e-09	6.9e-12	1.5e-13
4	7.416580102755271e-02	3.7e-03	2.8e-05	4.6e-09	6.7e-12	9.4e-15
5	7.840714643630796e-02	2.4e-04	2.0e-05	6.5e-09	6.6e-13	2.4e-14
6	5.345392880491968e-02	2.6e-03	1.6e-05	6.5e-09	9.6e-12	4.9e-14
7	2.611186407051911e-02	5.1e-03	6.8e-05	4.3e-09	8.6e-13	5.1e-14

[a] The run time was 23 s for the calculation of order 19.

Table 9. Results for the Profile of Figure 1a in TE Polarization With $h = 0.025$, $\lambda = 0.001$, and $\theta = 70°$[a]

Efficiency	Scattered Energy	Order 0	Order 1	Order 3	Order 7	Order 9
0	9.405896918172547e-03	9.1e-06	2.3e-07	1.2e-10	1.7e-14	6.1e-16
1	4.691450406852652e-03	1.2e-05	1.1e-07	8.4e-11	2.3e-16	2.2e-16
2	4.977619850889408e-03	1.2e-05	1.3e-07	7.3e-11	7.5e-15	9.1e-17
3	8.970028199252082e-03	1.1e-05	2.1e-07	1.8e-10	5.5e-15	3.6e-16
4	1.591650541515982e-03	8.4e-06	4.2e-08	2.5e-11	5.2e-17	3.9e-16
5	1.151449525094811e-02	6.0e-06	2.7e-07	2.7e-10	3.8e-15	5.7e-17
6	1.509705192413105e-04	2.8e-06	4.9e-09	8.3e-13	1.2e-15	2.0e-16
7	1.232860573339191e-02	6.3e-07	2.9e-07	3.5e-10	4.2e-15	7.6e-16

[a] The run time was 12 s for the order 9 calculation.

in equation (32) then yields

$$\sum_{n=-1}^{+\infty} \frac{1}{k^n}\left(\tilde{\nu}_n(x) - \frac{i}{2} I^n(x,\ k)\right) = 2k[i\sin(\theta) f'(x) + i\cos(\theta)], \tag{34}$$

where

$$I^n(x,k) = \int_{-\infty}^{+\infty} h(kr) g(x,x') \exp\{i\alpha(x'-x) - i\beta[f(x') - f(x)]\} \tilde{\nu}_n(x') dx'.$$

The solution of equation (34) requires asymptotic expansions for the integrals $I^n(x, k)$. These expansions are obtained, as in the TE case, by the methods of section 3. In particular, we obtain the following expressions for the coefficients $\tilde{\nu}_n(x)$:

$$\begin{cases} \tilde{\nu}_{-1}(x) = 2[i\sin(\theta) f'(x) + i\cos(\theta)] \\ \tilde{\nu}_n(x) = \dfrac{i}{2} \displaystyle\sum_{q=0}^{n} I_q^{n-q-1}(x). \end{cases} \tag{35}$$

7. Numerical Results

[30] Our numerical method proceeds to obtain the integral densities $\nu(x, k)$ through equation (6) in TE polarization and equation (33) in TM polarization, with coefficients ν_n and $\tilde{\nu}_n$ obtained from equations (9) and (35), respectively, and with I_q^n given by equation (25). The Taylor-Fourier expansions required in equation (12) for the functions ϕ_+^{-1} and g/ϕ_+' are precomputed, as they depend only on the profile f and they are independent of wave numbers, incidence angles, etc. The precomputation time was 0.5 s for the profile of Figure 1a and Figure 1b and 0.7 s for the profile of Figure 1c. (This and all subsequent calculations were performed in a DEC Alpha workstation (600 MHz).) Once the density has been obtained, all field-related quantities can be evaluated easily from equation (3) in the TE case and equation (29) in the TM case.

[31] In this section we present the results produced by our algorithm for the energy radiated in the various scattering directions. To do this, we use the periodic Green's function $\tilde{G}$ of period d [*Petit*, 1980]

$$\tilde{G}(x,y) = \frac{1}{2id} \sum_{n=-\infty}^{+\infty} \frac{e^{i\alpha - nx + i\beta ny}}{1\beta_n}, \quad \alpha_n = \alpha + n\frac{2\pi}{d}, \quad \beta_n = \sqrt{k^2 - \alpha_n^2}$$

to obtain from equation (3) (TE) or from equation (29) (TM) the Rayleigh series for the scattered field

$$u(x,y) = \sum_{n=-\infty}^{+\infty} B_n e^{i\alpha_n x + i\beta_n y}.$$

Table 10. Results for the Profile of Figure 1a in TM Polarization With $h = 0.025$, $\lambda = 0.0011$, and $\theta = 70°$[a]

Efficiency	Scattered Energy	Order 0	Order 1	Order 3	Order 7	Order 9
0	4.663322085313096e-03	2.9e-03	1.8e-05	1.4e-08	8.5e-14	9.9e-15
1	5.732453099268077e-03	2.4e-03	2.0e-05	1.5e-08	1.2e-14	1.0e-14
2	9.742422239435774e-03	1.4e-03	1.9e-05	1.5e-08	5.0e-14	2.7e-15
3	1.692802029774497e-03	5.8e-03	2.2e-05	1.7e-08	5.1e-16	2.9e-15
4	1.271613899298100e-02	5.4e-04	1.9e-05	1.7e-08	4.9e-14	2.5e-15
5	9.550848574956618e-05	2.7e-02	3.1e-05	2.7e-08	1.7e-13	8.7e-15
6	1.351161517190391e-02	2.2e-05	2.0e-05	1.9e-08	6.8e-14	5.3e-15
7	1.898341280339258e-04	2.0e-02	1.1e-05	9.9e-09	2.9e-13	7.6e-14

[a] The run time was 19 s for the order 9 calculation.

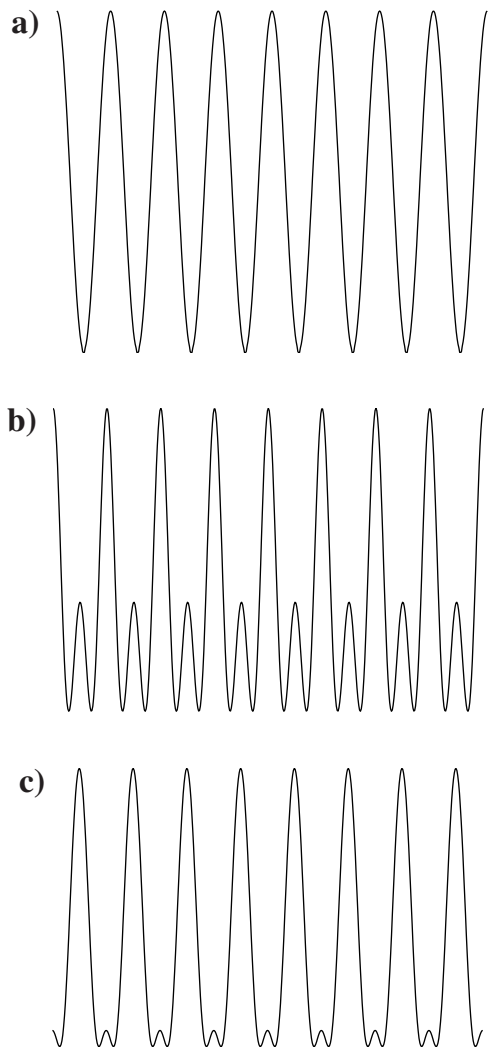

Figure 1. Various profiles considered in the text: (a) $f(x) = (h/2) \cos(2\pi x)$, (b) $f(x) = (h/2)[\cos(2\pi x) + \cos(4\pi x)]$, and (c) $f(x) = (h/2)[-\cos(2\pi x) + 0.35 \cos(4\pi x) - 0.035 \cos(6\pi x)]$.

Here, the coefficients B_n are "Rayleigh amplitudes," which are given in TE polarization by

$$B_n = \frac{1}{2d} \int_d^0 \left(-1 + \frac{\alpha_n}{\beta_n} f'(x) \right) \nu(x, k) e^{-i\alpha - nx - i\beta - nf(x)} dx.$$

and in TM polarization by

$$B_n = \frac{1}{2id\beta_n} \int_0^d \tilde{\nu}(x, k) e^{-i\alpha_n x - i\beta_n f(x)} dx.$$

The required integrals were computed by means of the trapezoidal rule, which for the periodic functions under consideration is spectrally accurate and can be computed very efficiently by means of the FFT.

[32] Our numerical results show values and errors corresponding to the "scattering efficiencies" e_n [see *Petit*, 1980], which are defined by

$$e_n = \frac{\beta_n}{\beta} |B_n|^2$$

and which give the fraction of the energy which is scattered in each one of the (finitely many) scattering directions. To test the accuracy of our numerical procedures, we compare our high-frequency (HF) results to those of the method of variation boundaries (MVB) [*Bruno and Reitich*, 1993a, 1993b, 1993c] in an "overlap" wavelength region, in which both algorithms are very accurate; additional results, in regimes beyond those that can be resolved by the boundary variation method, are also presented. Note that the HF and MVB methods are substantially different in nature: One is a high-order expansion in $1/k$ whereas the other is a high-order expansion in the height h of the profile. In Tables 2–10 we list relative errors for the computed values of scattered energies in the various scattering directions. The figures given in the columns denoted by orders 0–19 are the relative errors for the values of the scattered energy calculated from the high-frequency code to orders 0–19 in the corresponding scattering direction. In all cases, errors were evaluated through comparison with a highly accurate reference solution; in Tables 2–8 the reference solution was produced by means of the boundary variations code mentioned above; in Tables 9 and 10 the reference solution was obtained through a higher-order application of our high-frequency algorithm (order 15). The first term in the high-frequency expansion happens to coincide with the classical Kirchhoff approximation. Note that the Kirchhoff approximation can also be obtained as the zeroth-order term of the Neumann series for equation (4). We emphasize, however, that the high-frequency method used in this paper is of a completely different nature compared to that arising from use of Neumann series.

[33] Our first example, presented in Table 2, corresponds to the profile in Figure 1a illuminated by a TE-polarized plane wave with $h = 0.025$, $\lambda = 0.025$, and an incidence angle $\theta = 30°$. The run time was 10 s for the calculation of order 17; we see that, as claimed, the present approach produces results with full double precision accuracy in short computing times.

[34] The results for the profile in Figure 1a under TM polarization are given in Table 3. Here we take $h = 0.025$ and $\lambda = 0.0251$, with an incidence angle $\theta = 30°$. Our choice of wavelength in the present TM case, which is slightly different from the value $\lambda = 0.025$ we used in the TE case, was made to avoid the Wood anomaly [*Hutley*, 1982] that occurs at the latter value, for which the test boundary variation code fails. Our high-frequency method, however, does not suffer from that drawback, and results for the profile in Figure 1a with

$h = 0.025$, $\lambda = 0.025$, and an incidence angle $\theta = 30°$ are given in Table 4. The reference solution in this case is the high-order high-frequency solution of order 21. The convergence of our expansion in this case is similar to the convergence observed in the previous case where $\lambda/d = 0.0251$. Again, full double precision accuracies are reached in a 10 s calculation.

[35] Our method is not restricted to sinusoidal surfaces, of course. In Table 5, for instance, we present results corresponding to the profile of Figure 1b with $h = 0.01$, $\lambda = 0.025$, and $\theta = 0°$ in TE polarization. The run time was 5 s for the order 11 calculation. Table 6 shows results for the same profile under TM polarization with $h = 0.01$, $\lambda = 0.0251$, and $\theta = 0°$. The run time was 4 s for the order 11 calculation.

[36] We next consider the third-order "Stokes" wave [*Kinsman*, 1965] shown in Figure 1c. The results presented in Table 7 assumed the parameter values $h = 0.02$, $\lambda = 0.04$, and $\theta = 0°$ and TE polarization. The run time in this case was 27 s for the calculation of order 19. Table 8 shows the results for TM polarization and $h = 0.02$, $\lambda = 0.041$, and $\theta = 0°$. The run time was 23 s for the order 19 calculation.

[37] Table 9 presents results for a low grazing angle example for the profile of Figure 1a with $h = 0.025$, $\lambda = 0.001$, and $\theta = 70°$ (20° grazing) in TE polarization. As mentioned above, for reference in this case we used the high-frequency solution of order 15. The run time for the order 9 calculation was 12 s. The results for the profile of Figure 1a under TM polarization with $h = 0.025$, $\lambda = 0.0011$, and $\theta = 70°$ are given in Table 10. The run time was 19 s for the order 9 calculation.

[38] A final remark concerning the order of the Fourier series used in the examples above is now in order. For the examples given in Tables 2–8, no more than 30 Fourier modes were used. The number of Fourier modes needed depends on the incidence angle, the height of the profile, the order of the high-frequency expansion used, and the accuracy required; in the cases considered in Tables 9 and 10, for example, it was necessary to use 45 Fourier coefficients to achieve the accuracies reported.

8. Conclusions

[39] We have shown that high-order summations of expansions of the type of equation (1) can be used to produce highly accurate results for problems of scattering by rough surfaces in the high-frequency regime in TE and TM polarizations. Our algorithm is based on analytic continuation of divergent integrals and careful algebraic manipulation of Taylor-Fourier series representations. Our results show accuracies which improve substantially over those given by classical methods such as the Kirchhoff approximation. As shown recently [*Sei et al.*, 1999], such accuracies are needed to capture important aspects of rough surface scattering involving very low scattering returns and occurrences of unusual polarization ratios. Further, the results of *Bruno and Reitich* [1993a, 1993b, 1993c] clearly suggest that a multiscale perturbation algorithm of the type proposed by *Bruno et al.* [2000] should yield the required accuracies for multiscale surfaces provided that an accurate high-frequency solver, such as the one presented in this paper, is used. This paper thus extends the range of applicability of classical asymptotic methods, producing a versatile, highly accurate, and efficient high-frequency numerical solver.

[40] **Acknowledgments.** This effort was sponsored by DARPA/AFOSR under contract F49620-99-C-0014, by the Air Force Office of Scientific Research, Air Force Materials Command, USAF, under grants F49620-99-1-0010 and F49620-99-1-0193, and through NSF contracts DMS-9523292 and DMS-9816802. The views and conclusions contained herein are those of the authors and should not be interpreted as necessarily representing the official policies or endorsements, either expressed or implied, of the Air Force Office of Scientific Research or the U.S. Government.

References

Abramowitz, M., and I. Stegun, *Handbook of Mathematical Functions With Formulas, Graphs, and Mathematical Tables*, U.S. Dep. of Commer., Washington, D. C., June 1964.

Ahluwalia, D. S., R. M. Lewis, and J. Boersma, Uniform asymptotic theory of diffraction by a plane screen, *SIAM J. Appl. Math.*, *16*(4), 783–807, 1968.

Ansorge, H., Electromagnetic reflection from a curved dielectric interface, *IEEE Trans. Antennas Propag.*, *34*, 842–845, 1986.

Ansorge, H., First order corrections to reflection and transmission at a curved dielectric interface with emphasis on polarization properties, *Radio Sci.*, *22*, 993–998, 1987.

Benamou, J. D., Direct computations of multivalued phase space solutions for Hamilton-Jacobi equations, *Commun. Pure Appl. Math.*, *52*, 1443–1475, 1999.

Bleistein, N., and R. A. Handelsman, *Asymptotic Expansions of Integrals*, Dover, Mineola, N. Y., 1986.

Bloom, C. O., and N. D. Kazarinoff, *Short Wave Radiation Problems in Inhomogeneous Media: Asymptotic Solutions, Lect. Notes Math.*, vol. 522, Springer-Verlag, New York, 1976.

Bouche, D., F. Molinet, and R. Mittra, *Asymptotic Methods in Electromagnetics*, Springer-Verlag, New York, 1997.

Brown, W. P., On the asymptotic behavior of electromagnetic fields from convex cylinders near grazing incidence, *J. Math. Anal. Appl.*, *15*, 355–385, 1966.

Bruno, O., and F. Reitich, Numerical solution of diffraction problems: A method of variation of boundaries I, *J. Opt. Soc. Am. A Opt. Image Sci.*, *10*, 1168–1175, 1993a.

Bruno, O., and F. Reitich, Numerical solution of diffraction problems: A method of variation of boundaries II, *J. Opt. Soc. Am. A Opt. Image Sci.*, *10*, 2307–2316, 1993b.

Bruno, O., and F. Reitich, Numerical solution of diffraction problems: A method of variation of boundaries III, *J. Opt. Soc. Am. A Opt. Image Sci.*, *10*, 2551–2562, 1993c.

Bruno, O., A. Sei, and M. Caponi, Rigorous multi-scale solver for rough-surface scattering problems: High-order-high-frequency and variation of boundaries, paper presented at NATO Sensors and Electronics Technology (SET) Symposium on "Low Grazing Angle Clutter: Its Characterization, Measurement, and Application,"Appl. Phys. Lab., Johns Hopkins Univ., Laurel, Md., 25–27 April 2000.

Cartan, H., *Elementary Theory of Analytic Functions of One or Several Complex Variables*, Addison-Wesley-Longman, Reading, Mass., 1963.

Chaloupka, H., and H. J. Meckelburg, Improved high-frequency current approximation for curved conducting surfaces, *Arch. Elektron. Übertragungstech.*, *39*, 245–250, 1985.

Duistermaat, J. J., Huygens' principle for linear partial differential equations, in *Huygens' Principle, 1690–1990: Theory and Applications*, edited by H. Blok, pp. 273–297, Elsevier Sci., New York, 1992.

Fatemi, E., B. Engquist, and S. Osher, Numerical solution of the high frequency asymptotic expansion for the scalar wave equation, *J. Comput. Phys.*, *120*, 145–155, 1995.

Friedlander, F. G., Geometrical optics and Maxwell's equations, *Proc. Cambridge Philos. Soc.*, *43*(2), 284–286, 1946.

Friedlander, F. G., and J. B. Keller, Asymptotic expansion of solutions of $(\nabla^2 + k^2)u = 0$, *Commun. Pure Appl. Math.*, *8*, 387–394, 1955.

Gil'Man, M. A., A. G. Mikheyev, and T. L. Tkachenko, The two-scale model and other methods for the approximate solution of the problem of diffraction by rough surfaces, *USSR Comput. Math. Math. Phys., Engl. Transl.*, *36*, 1429–1442, 1996.

Hong, S., Asymptotic theory of electromagnetic and acoustic diffraction by smooth convex surfaces of variable curvature, *J. Math. Phys.*, *8*, 1223–1232, 1967.

Hutley, M. C., *Diffraction Gratings*, Academic, San Diego, Calif., 1982.

Keller, J. B., A geometric theory of diffraction, in *Calculus of Variations and Its Applications*, edited by L. M. Graves, pp. 27–52, McGraw-Hill, New York, 1958.

Kinsman, B., *Wind Waves, Their Generation and Propagation on the Ocean Surface*, Prentice-Hall, Old Tappan, N. J., 1965.

Kravtsov, Y. A., A modification of the geometric optics method, *Radiofizika*, *7*, 664–673, 1964.

Kuryanov, B. F., The scattering of sound at a rough surface with two types of irregularity, *Sov. Phys. Acoust., Engl. Transl.*, *8*(3), 252–257, 1963.

Lee, S. W., Electromagnetic reflection from a conducting surface: Geometrical optics solution, *IEEE Trans. Antennas Propag.*, *23*, 184–191, 1975.

Lewis, R. M., and J. Boersma, Uniform theory of edge diffraction, *J. Math. Phys.*, *10*, 2291–2305, 1969.

Lewis, R. M., and J. B. Keller, Asymptotic methods for partial differential equations: The reduced wave equation and Maxwell's equations, *Res. Rep. EM-194*, N. Y. Univ., New York, 1964. (Reprinted in *Surv. Appl. Math.*, *1*, 1–82, 1995).

Lewis, R. M., N. Bleistein, and D. Ludwig, Uniform asymptotic theory of creeping waves, *Commun. Pure Appl. Math.*, *20*, 295–320, 1967.

Ludwig, D., Uniform asymptotic expansion at a caustic, *Commun. Pure Appl. Math.*, *19*, 215–250, 1966.

Luneburg, R. K., *Mathematical Theory of Optics*, Brown Univ., Providence, R. I., 1944. (Reprinted by Univ. of Calif. Press, Berkeley, 1964.)

Luneburg, R. K., Asymptotic expansion of steady state electromagnetic fields, *Res. Rep. EM-14*, N. Y. Univ., New York, July 1949a.

Luneburg, R. K., Asymptotic evaluation of diffraction integrals, *Res. Rep. EM-15*, N. Y. Univ., New York, Oct. 1949b.

McDaniel, S. T., and A. D. Gorman, An examination of the composite-roughness scattering model, *J. Acoust. Soc. Am.*, *73*, 1476–1486, 1983.

Miranker, W. L., Parametric theory of $\Delta u + k^2 u$, *Arch. Ration. Mech. Anal.*, *1*, 139–152, 1957.

Mitzner, K. M., Effect of small irregularities on electromagnetic scattering from an interface of arbitrary shape, *J. Math. Phys.*, *5*, 1776–1786, 1964.

Petit, R., Ed., *Electromagnetic Theory of Gratings*, Springer-Verlag, New York, 1980.

Press, W. H., S. A. Teukolsky, W. T. Vetterling, and B. P. Flannery, *Numerical Recipes*, Cambridge Univ. Press, New York, 1992.

Rice, S. O., Reflection of electromagnetic waves from slightly rough surfaces, *Commun. Pure Appl. Math.*, *4*, 351–378, 1951.

Sei, A., O. P. Bruno, and M. Caponi, Study of polarization scattering anomalies with application to oceanic scattering, *Radio Sci.*, *34*, 385–411, 1999.

Shmelev, A. B., Wave scattering by statistically uneven surfaces, *Sov. Phys. Usp., Engl. Transl.*, *15*(2), 173–183, 1972.

Valenzuela, G. R., Theories for the interaction of electromagnetic and oceanic waves: A review, *Boundary Layer Meteorol.*, *13*, 61–85, 1978.

Van Kampen, N. G., An asymptotic treatment of diffraction problems, *Physica*, *14*(9), 575–589, 1949.

VanTrier, J., and W. W. Symes, Upwind finite- difference calculation of traveltimes, *Geophysics*, *56*, 812–821, 1991.

Vidale, J., Finite difference calculation of traveltimes, *Bull. Seismol. Soc. Am.*, *78*, 2062–2076, 1988.

Voronovich, A. G., *Wave Scattering From Rough Surfaces*, Springer-Verlag, New York, 1994.

O. P. Bruno, Applied Mathematics, California Institute of Technology, Pasadena, CA 91125, USA. (bruno@ama.caltech.edu)

M. Caponi and A. Sei, Ocean Technology Department, TRW, 1 Space Park, Redondo Beach, CA 90278, USA. (alain.sei@trw.com)